

**Degradable Polyanhydride Networks Derived from Itaconic  
Acid**

Journal:	<i>Polymer Chemistry</i>
Manuscript ID	PY-ART-09-2020-001388.R1
Article Type:	Paper
Date Submitted by the Author:	25-Nov-2020
Complete List of Authors:	Sajjad, Hussain; University of Minnesota, Chemistry Lillie, Leon; University of Minnesota, Chemistry; University of Minnesota Lau, Maggie; University of Minnesota, Chemical Engineering and Materials Science Ellison, Christopher; University of Minnesota, Chemical Engineering and Materials Science Tolman, William; Washington Univ Reineke, Theresa; University of Minnesota, Chemistry

# Degradable Poly(anhydride) Networks Derived from Itaconic Acid

*Hussnain Sajjad,<sup>a</sup> Leon M. Lillie,<sup>a</sup> C. Maggie Lau,<sup>b</sup> Christopher J. Ellison,<sup>b\*</sup> William B. Tolman,<sup>c\*</sup> and Theresa M. Reineke,<sup>a\*</sup>*

<sup>a</sup>Department of Chemistry and Center for Sustainable Polymers, University of Minnesota, Minneapolis, Minnesota 55455-0431.

<sup>b</sup>Department of Chemical Engineering and Materials Science, University of Minnesota, Minneapolis, Minnesota 55455-0431.

<sup>c</sup>Department of Chemistry, One Brookings Drive, Campus Box 1134, Washington University in St. Louis, St. Louis, MO 63130-4899.

\*Corresponding authors: [treineke@umn.edu](mailto:treineke@umn.edu), [wbtolman@wustl.edu](mailto:wbtolman@wustl.edu), [cellison@umn.edu](mailto:cellison@umn.edu)

KEYWORDS (itaconic acid, anhydride, thiol-ene photopolymerization, cycloaddition chemistry, norbornene, renewable, degradable)

## ABSTRACT

The development of tunable and degradable crosslinked-poly(anhydride) networks from renewably derived itaconic anhydrides and multifunctional thiols is presented. Itaconic acid was initially converted to ethyl itaconic anhydride and isoamyl itaconic anhydride via a two-step synthetic procedure on hundred-gram scale with minimal purification. Dinorbornene-functionalized derivatives were prepared via cycloaddition chemistry, and photoinitiated thiol-ene polymerization reactions were explored using commercially available tetra- and hexa-functional thiols, all using solvent-free syntheses. The thiol-ene reaction kinetics of different monomer compositions were characterized by real-time Fourier transform infrared (RT-FTIR) spectroscopy, with the norbornene functionalized derivatives exhibiting the highest reactivity towards thiol-ene photopolymerizations. The thermal and mechanical characteristics of the thermosets were analyzed and the viscoelastic behavior was investigated by dynamic mechanical

analysis to understand the influence of the ester functionality and choice of crosslinker on the material properties. The anhydride backbone was found to be susceptible to controlled degradation under physiologically- (phosphate-buffered saline) and environmentally-relevant (artificial seawater) testing conditions over a period of 60 days at 50 °C. This work demonstrates that itaconic acid may be a useful feedstock in the generation of degradable polyanhydride networks via thiol-ene photopolymerization.

## INTRODUCTION

Degradable polymers are an important class of materials that have found use in many applications such as drug carriers for controlled dosage release from within a biological matrix, implants for medical devices, and temporary scaffolds for regenerative tissue engineering systems.<sup>1-5</sup> Beyond biomedical applications, there is significant interest in using such polymers to create thermoplastic and networked materials that degrade in environmental conditions to reduce the accumulation of plastic waste.<sup>6</sup> Typically, the degradation profiles of such polymers are controlled by the presence of hydrolytically sensitive functionalities distributed throughout the material. For example, esters, hemiacetals, ortho esters, amides, disulfides, or glycosidic bonds are commonly employed to create degradable polymers.<sup>7-11</sup> Materials made from such polymers typically degrade via a bulk erosion mechanism, whereby hydrolytic degradation occurs throughout the entire polymer sample because the rate of water diffusion into the matrix is faster than the rate of bond hydrolysis.<sup>12,13</sup>

Polyanhydride materials exhibit fast rates of degradation over a wide range of conditions owing to the instability of the anhydride bonds relative to other functional groups.<sup>14,15</sup> As a consequence of their shorter hydrolysis half-lives, polyanhydrides also typically undergo a surface erosion mechanism because the rate of water diffusion into the matrix is slower than the

rate of bond cleavage at the interface. This property makes them ideal candidates for applications that require the controlled, steady release of bioactive compounds while maintaining their thermomechanical properties over the course of the degradation period. The commercial potential of such materials has been illustrated through the clinical use of the GLIADEL<sup>®</sup> wafer, a polyanhydride comprised of 1,3-bis(p-carboxyphenoxy)propane (CPP) and sebacic acid (SA), as an implantable release agent for brain cancer treatment.<sup>16</sup> Among the important benefits of polyanhydride materials for in vivo applications is their decomposition into non-toxic diacids.<sup>14</sup>

Despite these appealing advantages, polyanhydride use has been deterred by inconveniences in synthetic protocols and instability toward moisture, which complicates the logistics of transportation and storage.<sup>17</sup> Traditional synthetic routes for polyanhydrides have relied on condensation polymerizations, which require the use of harmful reagents or stringent conditions such as high heat and vacuum to remove condensates in order to achieve appreciable molecular weights.<sup>18,19</sup> More recent syntheses have used acrylic anhydride monomers for the production of photoinitiated, crosslinked polyanhydride networks.<sup>20–23</sup> However, such polymerizations are inhibited by oxygen, and the chain growth reaction results in the formation of materials with non-uniform crosslink densities. A significant improvement to this strategy relies on thiol-ene “click” chemistry to synthesize polyanhydride networks using vinyl anhydride monomers and multifunctional thiols.<sup>24–28</sup> Thiol-ene reactions are not oxygen inhibited and thus can be performed under ambient conditions.<sup>29,30</sup> The polymerizations can reach high conversions in relatively shorter timeframes, can be done without organic solvents, and can lead to more uniform crosslink densities due to the step-growth mechanism.

In addition to degradability, another goal for sustainable materials synthesis is to integrate renewable feedstocks in the production of materials with similar mechanical properties to

petroleum-based counterparts.<sup>6,31</sup> In pursuit of novel anhydride monomers that are useful for the synthesis of polyanhydride networks via thiol-ene polymerizations, we thus sought renewable feedstocks that can offer rich chemical functionalities for control over application-dependent properties. Towards this end, we aimed to produce tunable crosslinked polyanhydride networks from itaconic acid, a bio-derived feedstock. Itaconic acid, an unsaturated dicarboxylic acid, is currently obtained from the fermentation of biomass by *Aspergillus terreus*.<sup>32</sup> It is produced on an ever-expanding industrial scale (80 kiloton/yr) and is presently commercially available at \$1.8-2/kg.<sup>33,34</sup> Itaconic acid is analogous to vinyl monomers such as methacrylic acid, and has been applied to myriad applications ranging from resins, acrylate latexes, dispersants, to super-absorbent materials.<sup>35,36</sup> Notably, the acrylic functionality of itaconic acid has been previously used in post-polymerization modifications via thiol-ene chemistry.<sup>37</sup>

A challenge that must be overcome to use itaconic acid for radical-type polymerizations, however, is the low reactivity of its vinyl group, which is akin to bulky  $\alpha$ -substituted acrylates observed to undergo sluggish radical polymerizations.<sup>38,39</sup> To address this limitation, we sought to transform the relatively unreactive vinyl bond of itaconic acid into a functional group that is more amenable towards thiol-ene chemistry. Thiol-norbornene systems are known to follow a thiol-ene step-growth mechanism and at polymerization rates that are faster than various stoichiometric monomer systems.<sup>40</sup> The conversion of the vinyl group of itaconic acid to norbornene-functionalized monomers for use in ring-opening-metathesis polymerizations was previously established via cycloaddition chemistry with cyclopentadiene (CPD).<sup>37</sup>

Herein, we report the readily scalable synthesis of the linear itaconic anhydrides ethyl itaconic anhydride (**1**) and isoamyl itaconic anhydride (**2**), and subsequent conversion to dinorbornene-functionalized anhydrides (**3** and **4**) via efficient, solvent-free cycloaddition

chemistry. Photoinitiated thiol-ene polymerizations of **1** - **4** with commercially available multifunctional thiols were conducted under ambient conditions to form polyanhydride networks, and the relative rates and network conversions were examined by real-time FTIR. The thermal and mechanical characteristics of the networks were analyzed to elucidate structure-property relationships, and the hydrolytic stability of these materials was assessed under physiologically- and environmentally-relevant aqueous conditions. Here, we highlight itaconic acid as a valuable feedstock to create tunable and degradable polyanhydride networks via thiol-ene photopolymerization.

## RESULTS AND DISCUSSION

The initial inspiration for this work stems from the advantageously selective and high yielding monoesterification of itaconic acid.<sup>41</sup> This chemistry has been performed with a variety of alcohols, enabling facile modification of thermal and mechanical properties of the resultant materials. We postulated that these itaconic monoesters could be transformed to linear itaconic anhydrides using chemistry we previously used to make a monomer precursor, 10-undecenoic anhydride.<sup>42</sup> To the best of our knowledge, these itaconic acid-based anhydride structures are unexplored in the literature. The synthesis of itaconic anhydrides was accomplished from itaconic acid through a two-step synthesis (Figure 1, Supporting Information). The first step in the procedure involved the chemoselective esterification of itaconic acid with ethanol or isoamyl alcohol to produce ethyl itaconic acid (**1'**) and isoamyl itaconic acid (**2'**), respectively. The reactions were performed on large scales (100-200 g) with a single recrystallization step for purification. Both monoesters were then transformed into linear itaconic anhydrides by dehydration with acetic anhydride. The resultant anhydrides, ethyl itaconic anhydride (**1**) and isoamyl itaconic anhydride (**2**), were obtained as viscous oils with a slight yellow coloring.

Although we focused on the ethyl and isoamyl variants for this work, this methodology can be expanded to produce other linear ester itaconic anhydrides to modulate the physical and thermal properties, as well as the aqueous degradability profiles, of the polyanhydride networks.

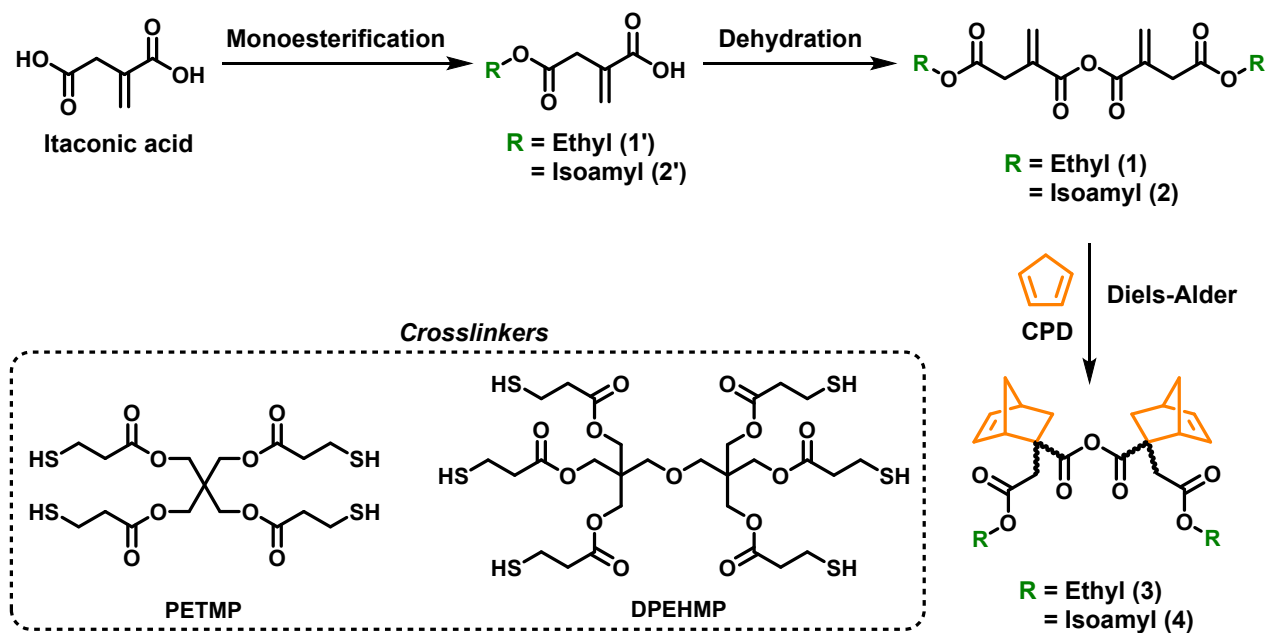


Figure 1. Synthetic scheme for the transformation of itaconic acid into the anhydride monomers used in this study (1 – 4) and multifunctional thiol crosslinkers pentaerythritol tetrakis(3-mercaptopropionate) (PETMP) and dipentaerythritol hexakis(3-mercaptopropionate) (DPEHMP) used in the formation of polyanhydride networks via thiol-ene chemistry.

Efficient cycloaddition reactions with cyclopentadiene were then used to convert **1** and **2** into the dinorbornene-functionalized anhydride monomers **3** and **4**. The reactions were performed without the use of organic solvents and with a small excess of CPD, and the products were purified in a single step to remove the excess CPD and dicyclopentadiene byproduct via vacuum distillation. The monomers **3** and **4** were produced as two sets of endo/exo diastereomers for each molecule, and these various possible endo/exo combinations convoluted the  $^1\text{H}$  NMR

spectra, making it challenging to integrate individual peaks in order to assess the purity of the monomer samples. To circumvent this issue and enable determination of the endo:exo ratios, the anhydride moieties in samples of **3** and **4** were hydrolyzed with trifluoroacetic acid at 100 °C to yield only one set of diastereomers (Figure 2). The resultant  $^1\text{H}$  NMR spectra, with signals that could be individually integrated, showed the samples to comprise pure monomers lacking any significant side-products. Integrations of the signals for the alkene protons showed an approximate 70:30 endo:exo ratio for both dinorbornene monomers, with the peaks assigned for the endo isomer on the basis of comparison to a similar norbornene monomer synthesized from itaconic acid reported in the literature.<sup>37</sup>

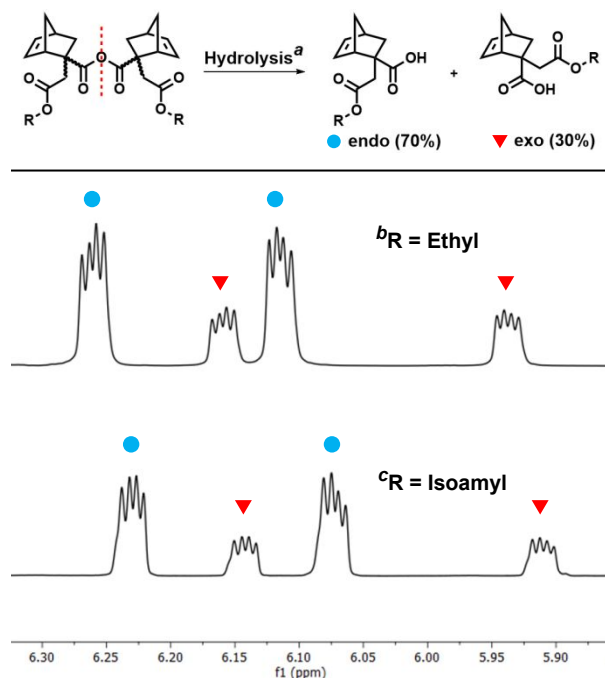


Figure 2. Acid-catalyzed hydrolysis of the dinorbornene-functionalized monomers to cleave the anhydride linkages. a) Samples of the anhydride monomers were dissolved in acetone- $d_6$  in NMR tubes with 100  $\mu\text{L}$  each of  $\text{D}_2\text{O}$  and trifluoroacetic acid. The sealed tubes were then heated at 100 °C for  $\sim 2$  h until complete hydrolysis of the anhydrides as monitored by  $^1\text{H}$  NMR. b)  $^1\text{H}$  NMR spectrum in the alkene region of the hydrolysis products of **3** and c)  $^1\text{H}$  NMR spectrum in the alkene region of the hydrolysis products of **4**. The blue circles indicate the alkene signals of the endo isomers and the red triangles indicate the alkene signals of the exo isomers.

The thiol-ene polymerization of the anhydride monomers **1** – **4** with multifunctional, commercially available thiols was monitored by real-time Fourier transform infrared (RT-FTIR) spectroscopy (Figure 3). Ensuring a 1:1 molar ratio of the ene:thiol end groups, the anhydride and thiol monomers were mixed together with 5 wt% of OMNIRAD TPO-L photoinitiator until a homogeneous solution was formed, and the samples were then placed between two polished NaCl plates. The Flory-Stockmayer theory (Equation 1) can be used to estimate the gel point ( $p_c$ ) of step-growth thiol-ene crosslinked networks, which is the point at which an infinite network is first established. In the equation,  $r$  is defined as the ratio of the thiol to ene functional groups and  $f$  is defined as the functionality of the thiol crosslinker component. With  $r = 1$  for all reaction mixtures (i.e. a 1:1 thiol:ene functionality ratio),  $f = 4$  for PETMP, and  $f = 6$  for DPEHMP,  $p_c$  was calculated to be 57.7% for networks using PETMP (indicated as a dashed red line) and 44.7% for networks using DPEHMP (indicated as a dotted red line). The reactions of **1** and **2** with pentaerythritol tetrakis(3-mercaptopropionate) (PETMP), following the conversion of the thiol group at  $2572\text{ cm}^{-1}$  as a function of irradiation time, were observed to be sluggish, approaching equilibrium at less than 10% conversion after 95 s. Additionally, the kinetic data based on the conversion of the C=C signal of **1** and **2** did not match that of the thiol signal (Figures S20 and S21, respectively). Theoretically, the conversion of the ene and thiol functional groups should be identical for a step-growth thiol-ene polymerization; instead, the conversion of alkene groups in **1** and **2** were higher at 40 – 45%. This observation implies that free-radical homopolymerization reactions of **1** and **2** complicate the desired thiol-ene reactions and lead to the formation of inhomogeneous network structures. Using a modified equation (Equation S1) for mixed chain- and step-growth thiol-ene polymerizations to calculate the gel point conversion for reactions of **1** and **2** with PETMP resulted in a C=C conversion of 21.6%.<sup>43</sup> Although the

results from the RT-FTIR experiments show C=C conversions for **1**-PETMP and **2**-PETMP above the theoretical polymerization gel point, we observed only the formation of viscous liquids following irradiation. While it is possible that the viscous liquids were “infinite” networks with conversions close to or above the theoretical gel point, it would be necessary to perform rheological measurements on the monomer mixture during the photopolymerization process to support that conclusion. Furthermore, the gel point conversion value is calculated based on an idealized theory that does not account for defects, such as loops and/or dangling ends, which may exist within the network. Regardless, use of monomers **1** and **2** in the thiol-ene photopolymerizations did not produce solidified materials, and we therefore focused our attention on the norbornene-functionalized monomers **3** and **4** for further studies.

$$(1) \quad p_c = \frac{1}{\sqrt{r[1 + (f - 2)]}}$$

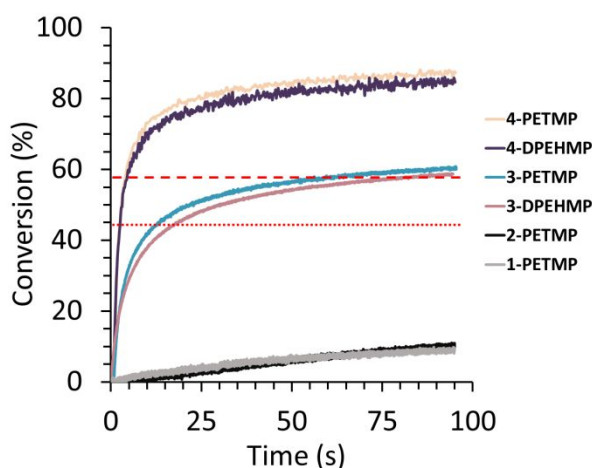


Figure 3. Conversions of the S-H functional groups in PETMP or DPEHMP determined by following the S-H signal at  $2572 \text{ cm}^{-1}$  in RT-FTIR experiments during photopolymerization reactions with anhydride monomers **1** – **4**. The dashed red line denotes the theoretical conversion at the gel point for thiol-ene step-growth networks formed with PETMP (57.7%) and similarly for the dotted red line with DPEHMP (44.7%).

The polymerization kinetic profiles of **3** and **4** with PETMP and dipentaerythritol hexakis(3-mercaptopropionate) (DPEHMP) show faster relative rates and higher conversions when compared to the profiles of **1** and **2**. It should be noted that the C=C vibrational frequency of the norbornene functional group was superimposed with other signals in the IR spectrum and thus S-H was monitored in the RT-FTIR experiments. The theoretical gel times (i.e. time to reach gel point) are 60 s and 3.9 s for **3**-PETMP and **4**-PETMP, respectively, and 18 s and 2.6 s, for **3**-DPEHMP and **4**-DPEHMP, respectively.

Monitoring the thiol peak as a function of irradiation time, **3**-PETMP reached a maximum conversion of 60% while **4**-PETMP reached 87% after 95 s. **3**-DPEHMP reached a maximum conversion of 59% while **4**-DPEHMP reached 85% after 95 s. As the enthalpy of reaction is expected to be similar for the two monomers (i.e. identical bonds are breaking and forming), the variations in conversion between **3** and **4** with PETMP and DPEHMP is attributed to the differences in mobility of the reactive functional groups within the polymer matrix during the reaction. Monomer mixtures that vitrify during polymerization are restricted in their molecular mobility at high conversions and, therefore, limited in the highest conversion that can be attained (i.e. a polymerization induced glass transition). Materials made with **4** exhibited glass transition temperatures ( $T_g$ ) below room temperature (discussed below), and thus, the materials were above their  $T_g$  during the polymerization and reached higher conversions. In the case of the materials made with **3**, the  $T_g$  values of the networks were above room temperature and, thus, these materials became vitrified during polymerization and could no longer react after that point. The improved reaction kinetics for the norbornene functionalized monomers **3** and **4** is a consequence of the thiol-ene reaction with norbornenes, which provides a significant relief in ring strain to the bicyclic structure. The carbon-centered radical that subsequently forms then undergoes rapid

hydrogen abstraction from thiols.<sup>44</sup> Norbornenes better adhere to stoichiometric step-growth polymerizations with thiols, resulting in greater consumption of reactive functional groups and, thus, higher conversions.<sup>40</sup> The results from the FT-IR studies demonstrate that conversion of the  $\alpha$ ,  $\beta$  unsaturated double bond of itaconic acid to norbornene groups was crucial in improving the reaction kinetics to form solid, crosslinked networks.

The thermal stability of the norbornene polyanhydride networks (**3**-PETMP, **3**-DPEHMP, **4**-PETMP, and **4**-DPEHMP) was analyzed via thermogravimetric analysis (TGA) at a heating rate of 10 °C min<sup>-1</sup> under a N<sub>2</sub> atmosphere up to 550 °C. The thermal decompositions of all four thermosets show nearly identical profiles, with decomposition temperatures (at 5% mass loss) in a narrow 230 – 242 °C range (Figure S22). The glass transition temperatures ( $T_g$ ) of the thermoset materials were determined by differential scanning calorimetry (DSC) at a heating ramp rate of 10 °C, and the reported thermograms were obtained from the second heating cycle to erase any thermal history (Figures S26 – S29). It is evident from the thermograms that all of the thermosets are amorphous, without any endothermic or exothermic peaks indicating the presence of crystalline domains. The  $T_g$  values of **3**-PETMP, **3**-DPEHMP, **4**-PETMP, and **4**-DPEHMP, are 26, 32, 16, and 21 °C, respectively. The  $T_g$  values of the thermosets formed from ethyl-based anhydrides were consistently higher than those formed from bulkier isoamyl-based anhydrides with the same thiol crosslinker, exemplifying how the thermal properties of the materials can be tuned by modifying the R group functionality of the ester bonds. Additionally, thermosets formed from DPEHMP showed higher  $T_g$  values than those formed from PETMP due to higher crosslinking densities. In comparison to similar polyanhydride networks made with 4-pentenoic acid and PETMP<sup>24,28</sup>, higher  $T_g$  polyanhydride networks were obtained with **3**-PETMP and **4**-PETMP. Incorporation of the rigid norbornene functionality within thiol-ene networks has

previously been shown to result high  $T_g$  materials.<sup>45</sup> The introduction of the norbornene moiety in monomers **3** and **4** is likely to be responsible for the comparatively higher  $T_g$  materials synthesized in this work.

Dynamic mechanical analysis (DMA) was performed on the thermosets to investigate their viscoelastic behavior as a function of temperature. The storage moduli and loss moduli are shown in Figure 4. The  $T_g$  of a crosslinked network can be recorded as the peak of the loss modulus as a function of temperature, identified as 26, 35, 17, and 23 °C, for **3**-PETMP, **3**-DPEHMP, **4**-PETMP, and **4**-DPEHMP, respectively. The plateau modulus in the rubbery plateau region was used to calculate the theoretical average molecular weight between points of crosslinking ( $M_c$ ) and crosslink density ( $\nu$ ) with Equations 2 and 3, where  $\rho$  is the mass density of the thermoset,  $E'$  is the plateau modulus at temperature  $T$ , and  $R$  is the universal gas constant. The results are summarized in Table 1, and the  $\nu$  values for **3**-PETMP, **3**-DPEHMP, **4**-PETMP, and **4**-DPEHMP were found to be 1.5, 3.5, 1.6, and 4.5  $\times 10^{-4}$  mol  $\text{cm}^{-3}$ . The calculated values only allow for a qualitative comparison among highly crosslinked networks,<sup>46</sup> which indicate that the crosslink densities of the materials are within the same order of magnitude.

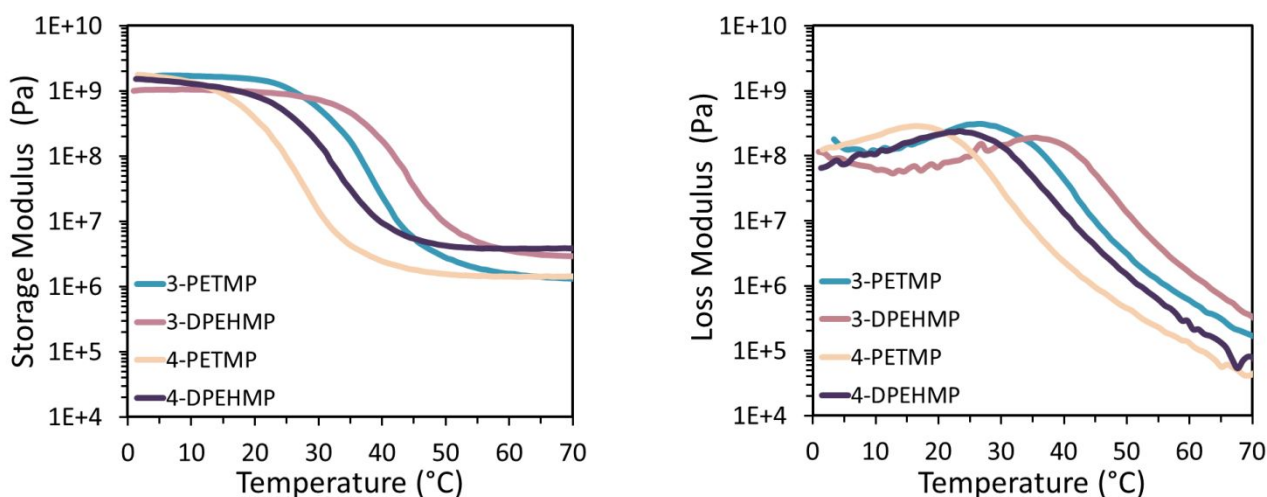


Figure 4. DMA data showing the storage moduli (left) and loss moduli (right) of the poly(amide) networks as a function of temperature.

$$M_c = \frac{3\rho RT}{E'} \quad (2)$$

$$\nu = \frac{\rho}{M_c} \quad (3)$$

Table 1. Summary of the characterization data for the polyanhydride networks studied in this work.

	3-PETMP	3-DPEHMP	4-PETMP	4-DPEHMP
$T_d$ (°C) <sup>a</sup>	236	242	240	230
$T_{g,DSC}$ (°C) <sup>b</sup>	23	32	17	21
$T_{g,DMA}$ (°C) <sup>c</sup>	26	35	17	23
$E$ (MPa) <sup>d</sup>	300 ± 36	560 ± 64	70 ± 10	260 ± 30
$E'$ (MPa) <sup>e</sup>	1.3	3.0	1.4	3.9
$\rho$ (g cm <sup>-3</sup> ) <sup>f</sup>	1.26	1.25	1.19	1.18
$M_c$ (g mol <sup>-1</sup> ) <sup>g</sup>	8300	3600	7300	2600
$\nu$ (mol cm <sup>-3</sup> ) <sup>h</sup>	1.5 x 10 <sup>-4</sup>	3.5 x 10 <sup>-4</sup>	1.6 x 10 <sup>-4</sup>	4.5 x 10 <sup>-4</sup>

<sup>a</sup>Degradation temperature at 5% weight loss. <sup>b</sup>Determined from the mid-point of the glass transition during the second heating ramp at 10 °C min<sup>-1</sup>. <sup>c</sup>Recorded as the temperature at the peak of the loss modulus data. <sup>d</sup>Young's modulus calculated from the first 2% elongation during uniaxial tensile testing. <sup>e</sup>Plateau modulus taken at 70 °C. <sup>f</sup>Mass density of the thermoset materials determined by Archimedes' principle with a density determination kit. <sup>g</sup>Calculated from eq 2 with  $T = 343$  K. <sup>h</sup>Calculated from eq 3.

The influence of the glass transition temperatures and crosslink densities on the mechanical behavior of the polyanhydride materials was assessed via uniaxial tensile analysis (Figure 5). Overall, the influence of both the glass transition temperature and crosslink densities must be considered in concert to understand the mechanical behavior of the materials. The stress at break and strain at break values, respectively, for the networks are as follows: 6.1 ± 0.8 MPa and 74 ±

9% for **3**-PETMP;  $8.8 \pm 1.1$  MPa and  $22 \pm 5\%$  for **3**-DPEHMP;  $4.7 \pm 0.5$  MPa for **4**-PETMP; and  $8.7 \pm 0.6$  and  $60 \pm 4\%$  for **4**-DPEHMP. **4**-PETMP, with a  $T_g$  below ambient temperature (ca.  $21$  °C) and a low crosslink density displayed the most elastomeric-like behavior with the lowest Young's modulus of  $70 \pm 10$  MPa. **3**-PETMP and **4**-DPEHMP exhibited similar Young's modulus values of  $300 \pm 36$  MPa and  $260 \pm 30$  MPa, respectively. Although **3**-PETMP had a lower crosslink density compared to **4**-DPEHMP, the fact that it has a higher  $T_g$  meant that the samples were in a vitrified state during tensile analysis. **4**-DPEHMP, comparatively, had a higher crosslink density but exhibited a  $T_g$  close to ambient temperature. **3**-DPEHMP, possessing the highest  $T_g$  and high crosslink density, displayed the most brittle behavior showing the highest ultimate tensile strength and largest Young's modulus value.

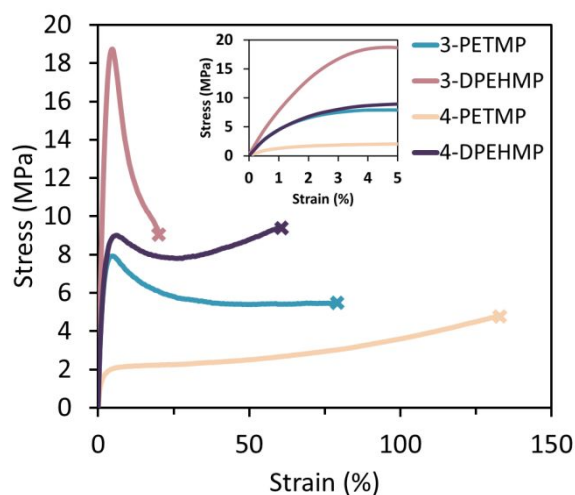


Figure 5. Representative engineering stress vs strain data for the polyanhydride networks. Samples were elongated at a rate of  $5 \text{ mm min}^{-1}$  until break (denoted with X). The inset shows the initial tensile behavior from 0 - 5% strain.

Interestingly, in our handling and testing of the polyanhydride networks, we observed that the materials gradually became brittle over the course of a week. In light of this observation,

thermal and physical characterization of the networks, discussed above, were performed immediately following photopolymerization (i.e. the same day). We hypothesized that the gradual change in material properties was due to chemical aging, where residual radicals in the crosslinked materials continue to react after photopolymerization.<sup>47-50</sup> Previous reports have demonstrated changes in physical properties after thermal curing following photopolymerization as a result of increased monomer consumption within the photocured materials.<sup>47-50</sup> Under this assumption, a sample of **3**-PETMP was photopolymerized in a quartz capillary tube and immediately subjected to electron paramagnetic resonance (EPR) spectroscopy. The acquired EPR spectrum (Figure S27) showed a signal that indicated the presence of radicals in the polymer matrix. It is uncertain at this time which radical species (e.g. thiyl radicals and/or carbon-based radicals) gave rise to the EPR signal. The sample was then thermally treated at 100 °C for 24 h to accelerate the consumption of the residual radicals, and then again subjected to EPR spectroscopy. The newly acquired EPR spectrum was observed to be silent (Figure S28), indicating that the radical species were quenched. In a parallel experiment, a photopolymerized sample was left to anneal at ambient temperature (22 °C) for three days and then also subjected to EPR spectroscopy. The acquired EPR spectrum was nearly silent. In order to determine the ultimate thermal and viscoelastic properties, samples of the polyanhydride networks were thermally treated at 100 °C for 24 after photopolymerization and then analyzed via DSC (Figures S29 – S32) and DMA (Figures S33 – S36) (Table 2). The results, summarized in Table 2, showed an increase in  $T_g$  for **3**-PETMP, **3**-DPEHMP, **4**-PETMP, and **4**-DPEHMP to 34, 38, 24, and 29 °C, respectively. While DMA indicated an increase in the plateau moduli of the materials, the ultimate  $\nu$  values for **3**-PETMP, **3**-DPEHMP, **4**-PETMP, and **4**-DPEHMP were calculated to be 1.9, 4.4, 2.1, and  $6.4 \times 10^{-4}$  mol cm<sup>-3</sup>, which are on the same order of magnitude as the

samples before thermal treatment. Reiterating that only a qualitative analysis can be made for highly crosslinked materials, the results indicate that the crosslink densities do not significantly increase as a result of chemical aging. Tensile analysis after the thermal treatment could not be performed due to the brittle nature of the materials.

Table 2. Summary of the characterization data for the polyanhydride networks after thermal treatment.

	3-PETMP <sup>a</sup>	3-DPEHMP <sup>a</sup>	4-PETMP <sup>a</sup>	4-DPEHMP <sup>a</sup>
$T_{g,DSC}$ (°C) <sup>b</sup>	34	37	23	27
$T_{g,DMA}$ (°C) <sup>c</sup>	34	38	24	29
$E'$ (MPa) <sup>d</sup>	1.6	3.8	1.8	5.5
$\rho$ (g cm <sup>-3</sup> ) <sup>e</sup>	1.26	1.25	1.19	1.18
$M_c$ (g mol <sup>-1</sup> ) <sup>f</sup>	6700	2800	5600	1800
$\nu$ (mol cm <sup>-3</sup> ) <sup>g</sup>	1.9 x 10 <sup>-4</sup>	4.4 x 10 <sup>-4</sup>	2.1 x 10 <sup>-4</sup>	6.4 x 10 <sup>-4</sup>

<sup>a</sup>Thermal data and viscoelastic properties measured after thermal treatment at 100 °C for 24 h.

<sup>b</sup>Determined from the mid-point of the glass transition in DSC during the second heating ramp at 10 °C min<sup>-1</sup>. <sup>c</sup>Recorded as the temperature at the peak of the loss modulus data. <sup>d</sup>Plateau modulus at taken at 70 °C. <sup>e</sup>Mass density of the thermoset materials. <sup>f</sup>Calculated from eq 2 with  $T = 343$  K. <sup>g</sup>Calculated from eq 3.

Finally, the aqueous degradation profiles of the polyanhydride networks were assessed in deionized (DI) water (pH 7.0) as well as biologically-relevant (phosphate buffered salt (PBS) solution, pH 7.4) and environmentally-relevant (artificial sea water (SW), pH 7.8) conditions. Initial degradation studies conducted at room temperature revealed that the materials were stable in all tested aqueous environments, with less than 10% mass loss occurring after a month of testing (Figure S37). Similar polyanhydride networks, such as those made from 4-pentenoic

anhydride and PETMP<sup>24-28</sup>, have been reported to degrade in aqueous environments within 1 – 3 days under ambient or physiological conditions ( $\leq 37$  °C, DI water or PBS solution). The more hydrophobic molecular structure of the itaconic acid-based anhydride monomers synthesized in this work, containing dinorbornene units and alkyl ester substituents, is likely responsible for the comparatively prolonged stability to moisture and aqueous environments we have observed. At elevated temperatures (e.g. 50 °C), however, the degradation processes was accelerated (Figure 6). The materials were found to slowly degrade in DI water at 50 °C, with approximately 20% mass loss for **4**-PETMP and **4**-DPEHMP and approximately 50% mass loss for **3**-PETMP and **4**-DPEHMP occurring after 51 days. Faster rates of degradation were observed in the buffered conditions of PBS solution and artificial SW at 50 °C. Complete degradation of the materials in PBS solution occurred within 24 – 37 days, and longer exposure times of 37 – 51 days were required to completely degrade the materials in artificial SW. We attribute the difference in rates of degradation between the PBS solution and artificial SW to the difference in buffering capacity of the aqueous media. While artificial SW had a higher initial pH than the PBS solution (7.8 vs 7.4), pH measurements of the solutions after complete degradation of the materials revealed that the PBS solutions maintained the highest pH (Table S1). The higher buffering capacity of the PBS solution can allow for better neutralization and solubilization of the network decomposition products while maintaining higher pH values, resulting in faster degradation rates. The prolonged stability of the anhydride networks under ambient conditions and aqueous environments is advantageous as it can allow for storage of these materials under ambient conditions without significant deterioration, and then can be degraded at elevated temperatures. Additionally, the materials were observed to degrade via a surface erosion mechanism, exhibiting a gradual loss in size during the course of the degradation experiments. It should be emphasized that while we

focused on the ethyl and isoamyl variants of the anhydride monomers for this study, the ester functionality can be tuned with other substituents with varying degrees of hydrophobicity or hydrophilicity with the potential to allow for control over the rate of degradation. Additionally, the effects of thiol and thio-ester degradation byproducts on the environment must be taken into consideration when designing degradable materials. While toxicological studies were outside the scope of the current work, future studies will assess the environmental impacts of such products.

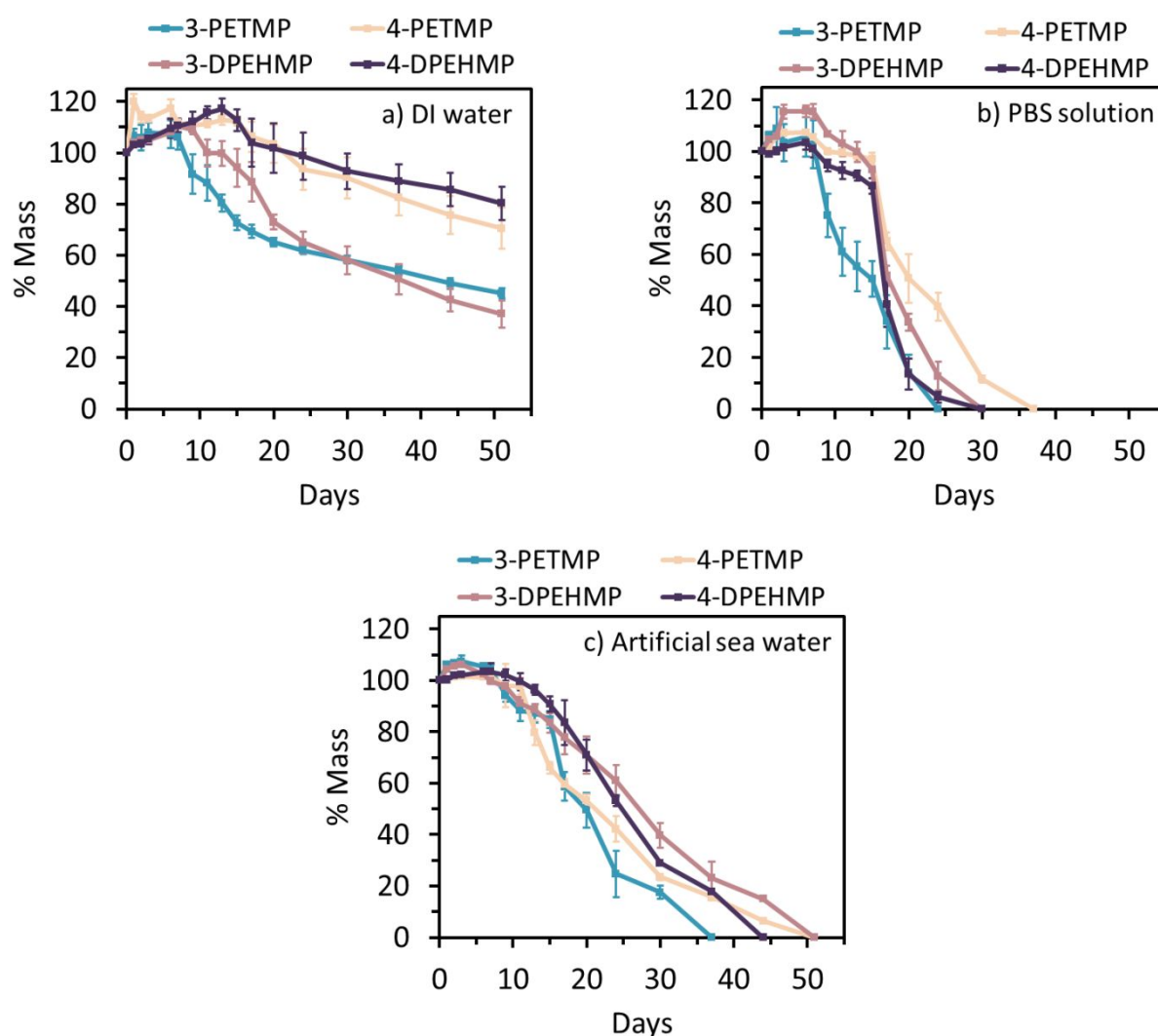


Figure 6. Hydrolytic stability tests of the polyanhydride networks at 50 °C in a) DI water (pH 7.0), b) phosphate buffer saline (PBS) solution (pH 7.4), and c) artificial sea water (7.8). Each vertex in the degradation profiles represents the average mass of samples in triplicate.

In summary, we described the facile and scalable synthesis of novel linear anhydrides with tunable ester functionalities from itaconic acid. The photoinitiated thiol-ene polymerization of the anhydrides to form crosslinked polyanhydride networks was accomplished with commercially available tetrafunctional and hexafunctional thiols. The ester functionality of the anhydride monomers was found to have an influence on the degree of polymerization, with the bulkier isoamyl variant reaching higher conversions than the ethyl variant possibly as a consequence of greater free volume within the polymer matrix during polymerization. Use of the higher functionality hexathiol crosslinker DPEHMP yielded stiffer, higher  $T_g$  materials than those made with the tetrafunctional thiol PETMP. The polyanhydride networks were susceptible to degradation in aqueous environments, and the results indicated that buffered solutions that are able to maintain a more basic environment resulted in faster degradation rates. Future studies are aimed at investigating the effect of hydrophobic and hydrophilic ester substituents on the rates of degradation, as we postulate that degradation profiles of the networks can also be controlled by modulating the structure of the anhydride monomers. Findings from this work demonstrate a viable strategy to potentially address micro-plastics pollution through the development of renewable polyanhydride networks from itaconic acid that degrade in aqueous environments.

## **AUTHOR INFORMATION**

### **Corresponding Author**

\*E-mail: [treineke@umn.edu](mailto:treineke@umn.edu), [wbtolman@wustl.edu](mailto:wbtolman@wustl.edu)

### **Notes**

The authors declare no competing financial interest.

## **ACKNOWLEDGMENT**

This work was supported by the National Science Foundation under the Center for Sustainable Polymers (CHE-1901635) and by the National Science Foundation Graduate Research Fellowship Program (to C.M. Lau) under Grant No. DGE-1348264. Any opinions, findings, and conclusions or recommendations expressed in this material are those of the author(s) and do not necessarily reflect the views of the National Science Foundation.

## REFERENCES

- (1) Lendlein, A.; Sisson, A. *Handbook of Biodegradable Polymers: Isolation, Synthesis, Characterization and Applications*; Wiley-VCH Verlag GmbH & Co. KGaA, 2011.
- (2) Kamaly, N.; Yameen, B.; Wu, J.; Farokhzad, O. C. Degradable Controlled-Release Polymers and Polymeric Nanoparticles: Mechanisms of Controlling Drug Release. *Chem. Rev.* **2016**, *116*, 2602-2663.
- (3) Uhrich, K. E.; Cannizzaro, S. M.; Langer, R. S.; Shakesheff, K. M. Polymeric Systems for Controlled Drug Release. *Chem. Rev.* **1999**, *99*, 3181-3198.
- (4) Zhang, Z.; Ortiz, O.; Goyal, R.; Kohn, J. Biodegradable Polymers. In *Principles of Tissue Engineering: Fourth Edition*; Elsevier, 2013, 441-473.
- (5) Jothimani, B.; Venkatachalapathy, B.; Karthikeyan, N. S.; Ravichandran, C. A Review on Versatile Applications of Degradable Polymers. In *Green Biopolymers and their Nanocomposites*; Springer, Singapore, 2019, 403-422.
- (6) Zhu, Y.; Romain, C.; Williams, C. K. Sustainable Polymers from Renewable Resources. *Nature* **2016**, *540*, 354-362.
- (7) Vroman, I.; Tighzert, L. Biodegradable Polymers. *Materials* **2009**, *2*, 307-344.

- (8) Luckachan, G. E.; Pillai, C. K. S. Biodegradable Polymers- A Review on Recent Trends and Emerging Perspectives. *J. Polym. Environ.* **2011**, *19*, 637-676.
- (9) Jiang, L.; Zhang, J. Biodegradable Polymers and Polymer Blends. In *Handbook of Biopolymers and Biodegradable Plastics: Properties, Processing and Applications*; Elsevier, 2013, 109-128.
- (10) Gunatillake, P. A.; Adhikari, R.; Gadegaard, N. Biodegradable Synthetic Polymers for Tissue Engineering. *Eur Cell Mater.* **2003**, *5*, 1-16.
- (11) Herwig, G.; Dove, A. P. Synthesis of Rapidly Surface Eroding Polyorthoesters and Polyacetals Using Thiol-Ene Click Chemistry. *ACS Macro Lett.* **2019**, *8*, 1268-1274.
- (12) Göpferich, A. Mechanisms of Polymer Degradation and Erosion. *Biomaterials* **1996**, *17*, 103-114.
- (13) Burkersroda, F. Von; Schedl, L.; Göpferich, A. Why Degradable Polymers Undergo Surface Erosion or Bulk Erosion. *Biomaterials* **2002**, *23*, 4221-4231.
- (14) Kumar, N.; Langer, R. S.; Domb, A. J. Polyanhydrides: An Overview. *Adv. Drug Deliv. Rev.* **2002**, *54*, 889-910.
- (15) Basu, A.; Domb, A. J. Recent Advances in Polyanhydride Based Biomaterials. *Adv. Mater.* **2018**, *30*, 1706815.
- (16) Dang, W.; Daviau, T.; Ying, P.; Zhao, Y.; Nowotnik, D.; Clow, C. S.; Tyler, B.; Brem, H. Effects of GLIADEL® Wafer Initial Molecular Weight on the Erosion of Wafer and Release of BCNU. *J. Control. Release* **1996**, *42*, 83-92.

- (17) Deronde, B. M.; Carbone, A. L.; Uhrich, K. Storage Stability Study of Salicylate-Based Poly(Anhydride-Esters). *Polym. Degrad. Stab.* **2010**, *95*, 1778-1782.
- (18) Leong, K. W.; Simonte, V.; Langer, R. Synthesis of Poly(anhydrides): Melt-Polycondensation, Dehydrochlorination, and Dehydrative Coupling. *Macromolecules* **1987**, *20*, 705-712.
- (19) Uhrich, K. E.; Gupta, A.; Thomas, T. T.; Laurencin, C. T.; Langer, R. Synthesis and Characterization of Degradable Poly(Anhydride-Co-Imides). *Macromolecules* **1995**, *28*, 2184-2193.
- (20) Muggli, D. S.; Burkoth, A. K.; Keyser, S. A.; Lee, H. R.; Anseth, K. S. Reaction Behavior of Biodegradable, Photo-Cross-Linkable Poly(anhydrides). *Macromolecules* **1998**, *31*, 4120-4125.
- (21) Anseth, K. S.; Shastri, V. R.; Langer, R. Photopolymerizable Degradable Poly(anhydrides) with Osteocompatibility. *Nat. Biotechnol.* **1999**, *17*, 156-159.
- (22) Tarcha, P. J.; Su, L.; Baker, T.; Langridge, D.; Shastri, V.; Langer, R. Stability of Photocurable Anhydrides: Methacrylic Acid Mixed Anhydrides of Nontoxic Diacids. *J. Polym. Sci. Part A Polym. Chem.* **2001**, *39*, 4189-4195.
- (23) Burkoth, A. K.; Anseth, K. S. A Review of Photocrosslinked Poly(anhydrides): In Situ Forming Degradable Networks. *Biomaterials* **2000**, *21*, 2395-2404.
- (24) Rutherglen, B. G.; McBath, R. A.; Huang, Y. L.; Shipp, D. A. Poly(anhydride) Networks from Thiol-Ene Polymerizations. *Macromolecules* **2010**, *43*, 10297-10303.
- (25) Shipp, D. A.; McQuinn, C. W.; Rutherglen, B. G.; McBath, R. A. Elastomeric and

- Degradable Polyanhydride Network Polymers by Step-Growth Thiol-Ene Photopolymerization. *Chem. Commun.* **2009**, *42*, 6415-6417.
- (26) Poetz, K. L.; Mohammed, H. S.; Snyder, B. L.; Liddil, G.; Samways, D. S. K.; Shipp, D. A. Photopolymerized Cross-Linked Thiol-Ene Polyanhydrides: Erosion, Release, and Toxicity Studies. *Biomacromolecules* **2014**, *15*, 2573-2582.
- (27) Poetz, K. L.; Durham, O. Z.; Shipp, D. A. Polyanhydride Nanoparticles by “click” Thiol-Ene Polymerization. *Polym. Chem.* **2015**, *6*, 5464-5469.
- (28) Poetz, K. L.; Mohammed, H. S.; Shipp, D. A. Surface Eroding, Semicrystalline Polyanhydrides via Thiol-Ene “Click” Photopolymerization. *Biomacromolecules* **2015**, *16*, 1650-1659.
- (29) Hoyle, C. E.; Bowman, C. N. Thiol-Ene Click Chemistry. *Angew. Chem. Int. Ed.* **2010**, *49*, 1540-1573.
- (30) Lowe, A. B. Thiol-Ene “Click” Reactions and Recent Applications in Polymer and Materials Synthesis: A First Update. *Polym. Chem.* **2014**, *5*, 4820-4870.
- (31) Lambert, S.; Wagner, M. Environmental Performance of Bio-Based and Biodegradable Plastics: The Road Ahead. *Chem. Soc. Rev.* **2017**, *46*, 6855-6871.
- (32) Okabe, M.; Lies, D.; Kanamasa, S.; Park, E. Y. Biotechnological Production of Itaconic Acid and Its Biosynthesis in *Aspergillus Terreus*. *Appl Microbiol Biotechnol.* **2009**, *84*, 597-606.
- (33) Werpy, T.; Petersen, G. *Top Value Added Chemicals from Biomass: Volume I -- Results of Screening for Potential Candidates from Sugars and Synthesis Gas*. United States, 2004.

- (34) Bafana, R.; Pandey, R. A. New Approaches for Itaconic Acid Production: Bottlenecks and Possible Remedies. *Critical Reviews in Biotechnology*. **2018**, *38*, 68-82.
- (35) Kumar, S.; Krishnan, S.; Samal, S. K.; Mohanty, S.; Nayak, S. K. Itaconic Acid Used as a Versatile Building Block for the Synthesis of Renewable Resource-Based Resins and Polyesters for Future Prospective: A Review. *Polym. Int.* **2017**, *66*, 1349-1363.
- (36) Robert, T.; Friebel, S. Itaconic Acid-a Versatile Building Block for Renewable Polyesters with Enhanced Functionality. *Green Chem.* **2016**, *18*, 2922-2934.
- (37) Winkler, M.; Lacerda, T. M.; Mack, F.; Meier, M. A. R. Renewable Polymers from Itaconic Acid by Polycondensation and Ring-Opening-Metathesis Polymerization. *Macromolecules* **2015**, *48*, 1398-1403.
- (38) Penelle, J.; Collot, J.; Rufflard, G. Kinetic and Thermodynamic Analysis of Methyl Ethacrylate Radical Polymerization. *J. Polym. Sci. Part A Polym. Chem.* **1993**, *31*, 2407-2412.
- (39) Trotta, J. T.; Jin, M.; Stawiasz, K. J.; Michaudel, Q.; Chen, W. L.; Fors, B. P. Synthesis of Methylene Butyrolactone Polymers from Itaconic Acid. *J. Polym. Sci. Part A Polym. Chem.* **2017**, *55*, 2730-2737.
- (40) Cramer, N. B.; Reddy, S. K.; O'Brien, A. K.; Bowman, C. N. Thiol - Ene Photopolymerization Mechanism and Rate Limiting Step Changes for Various Vinyl Functional Group Chemistries. *Macromolecules* **2003**, *36*, 7964-7969.
- (41) Cowie, J. M. G.; Hag, Z. Poly(mono n-alkyl itaconic acid esters): Their preparation and some physical properties. *Polym. Inter.* **1977**, *9*, 241-245.

- (42) Lillie, L. M.; Tolman, W. B.; Reineke, T. M. Structure/Property Relationships in Copolymers Comprising Renewable Isosorbide, Glucarodilactone, and 2,5-Bis(Hydroxymethyl)Furan Subunits. *Polym. Chem.* **2017**, *8*, 3746-3754.
- (43) Reddy, S. K.; Okay, O.; Bowman, C. N. Network Development in Mixed Step-Chain Growth Thiol-Vinyl Photopolymerizations. *Macromolecules* **2006**, *39*, 8832-8843.
- (44) Hoyle, C. E.; Lee, T. Y.; Roper, T. Thiol-Enes: Chemistry of the Past with Promise for the Future. *J. Polym. Sci. Part A Polym. Chem.* **2004**, *42*, 5301-5338.
- (45) Carioscia, J.A.; Schneidewin, L.; O'Brien, C.; Cramer, N.; Bowman, C. N. Thiol-Norbornene Materials: Approaches to Develop High  $T_g$  Thiol-Ene Polymers. *J. Polym. Sci. Part A Polym. Chem.* **2007**, *45*, 5686-5696.
- (46) Hiemenz, P. C., Lodge, T. P. *Polymer Chemistry*; CRC Press, 2007.
- (47) Lovell, L. G.; Berchtold, K. A.; Elliott, J. E.; Lu, H.; Bowman, C. N. Understanding the Kinetics and Network Formation of Dimethacrylate Dental Resins. *Polym. Adv. Technol.* **2001**, *12*, 335-345.
- (48) Scott, T. F.; Cook, W. D.; Forsythe, J. S.; Bowman, C. N.; Berchtold, K. A. FTIR and ESR Spectroscopic Studies of the Photopolymerization of Vinyl Ester Resins. *Macromolecules* **2003**, *36*, 6066-6074.
- (49) Berchtold, K. A.; Randolph, T. W.; Bowman, C. N. Propagation and Termination Kinetics of Cross-Linking Photopolymerizations Studied Using Electron Paramagnetic Resonance Spectroscopy in Conjunction with near IR Spectroscopy. *Macromolecules* **2005**, *38*, 6954-6964.

- (50) Lovestead, T. M.; Berchtold, K. A.; Bowman, C. N. An Investigation of Chain Length Dependent Termination and Reaction Diffusion Controlled Termination during the Free Radical Photopolymerization of Multivinyl Monomers. *Macromolecules* **2005**, *38*, 6374-6381.

TOC Graphic:

